Volume 1 | Number 1 | Jan 2013 | Pages 1–100

Dalton Transactions

An international journal of inorganic chemistry
www.rsc.org/dalton

ROYAL SOCIETY OF CHEMISTRY

ROYAL SOCIETY OF CHEMISTRY

www.rsc.org/dalton

Table of contents entry

Efficient NO photorelease in *cis*(Cl,Cl)-[Ru^{II}(FT)Cl$_2$(NO)](PF$_6$) and *trans*(Cl,Cl)-[Ru^{II}(FT)Cl$_2$(NO)](PF$_6$) with a quantum yield of 0.31 and 0.10 respectively has been explored by means of theoretical, photophysical and electrochemical analyses

Comparative photo-release of nitric oxide from isomers of substituted terpyridinenitrosylruthenium(II) complexes: experimental and computational investigations.

Joëlle Akl,[a] Isabelle Sasaki,[a] Pascal G. Lacroix,[a]* Isabelle Malfant,[a]* Sonia Mallet-Ladeira,[a] Patricia Vicendo,[b] Norberto Farfán,[c] and Rosa Santillan.[d]

Abstract

The 4'-(2-fluorenyl)-2,2':6',2''-terpyridine (FT) ligand and its *cis*(Cl,Cl)- and *trans*(Cl,Cl)-$[Ru^{II}(FT)Cl_2(NO)](PF_6)$ complexes have been synthesized. Both isomers were separated by HPLC and fully characterized by ^1H and ^{13}C NMR. The X-Ray diffraction crystal structures were solved for FT (Pna2$_1$ space group, a = 34.960(4), b = 5.9306(7), c = 9.5911(10) Å), and *trans*(Cl,Cl)-$[Ru^{II}(FT)Cl_2(NO)](PF_6)$·MeOH (P-1 space group, a = 10.3340(5), b = 13.0961(6), c = 13.2279(6) Å, α = 72.680(2), β = 70.488(2), γ = 67.090(2) deg.). Photo-release of NO$^•$ radicals occurs under irradiation at 405 nm, with a quantum yield of 0.31 and 0.10 for *cis*(Cl,Cl)-$[Ru^{II}(FT)Cl_2(NO)](PF_6)$, and *trans*(Cl,Cl)-$[Ru^{II}(FT)Cl_2(NO)](PF_6)$, respectively. This significant difference is likely due to the *trans* effect of Cl$^-$, which favors the photo-release. UV-visible spectroscopy and cyclic voltammetry indicate the formation of ruthenium(III) species as photoproducts. A density functional theory (DFT) analysis provides a rationale for the understanding of the photo-physical properties, and allows relating the weakening of the Ru-NO bond, and finally the photo-dissociation, to HOMO $\rightarrow$ LUMO excitations.

[a] Laboratoire de Chimie de Coordination du CNRS, 205 route de Narbonne, F-31077 Toulouse, France.
[b] Laboratoire des Interactions Moléculaires et de la Réactivité Chimique et Photochimique, Université Paul Sabatier 118 route de Narbonne, F-31062 Toulouse, France.
[c] Facultad de Química, Departamento de Química Orgánica, Universidad Nacional Autónoma de México, 04510 México D.F., México.
[d] Departamento de Química, Centro de Investigación y de Estudios del IPN, CINVESTAV, Apdo., Postal 14-740, México, D.F., 07000, México.

1

Introduction

The past three decades have witnessed an ever increasing interest for nitric oxide (NO), which has been recognized to possess a wide variety of physiological and pathological functions.[1,2] Depending on its concentration in human tissues, NO can affect vasodilatation,[1,3] and neurotransmission in the brain,[4] or lead to apoptosis (programmed cell death) and inhibition of tumor growth.[5-7] Since these discoveries, many research efforts have been directed towards the development of exogenous NO donors, capable of NO delivery in specific targets. Among them, metal (Fe,[8] Mn,[9] Cr,[10] and Ru[11]) nitrosyls have provided the most promising candidates. Ruthenium nitrosyls are especially appealing in relation to their inherent stability in aqueous media, compared to most alternative metal complexes.[12] Indeed, they release NO only when exposed to light, which makes them candidates of choice with the advent of photodynamic therapy (PDT), which allows the drug delivery to occur specifically in targeted cells on which the light irradiation can be focused.[13-16] Along this line, any ruthenium nitrosyl complex exhibiting an intense photosensitivity becomes interesting candidate for NO release.

These last few years, various metal-nitrosyl [M-NO] complexes have been reported in the literature in which a light induced isomerization can take place in solid state as follows:[17-21]

$$[M-NO] \leftrightarrow [M-ON] \qquad (1)$$

Light induced metal nitrosyl isomerization is an alternative property which reflects the photo-sensibility of NO in a specific environment. For more than 30 years, the highest population of light-induced [M-ON] metastable state ever reported was 50 % in a crystal of $Na_2[Fe(CN)_5(NO)] \cdot 2H_2O$ (sodium nitroprusside).[22] However, we have recently observed that the $[Ru^{II}(py)_4Cl(NO)](PF_6)_2 \cdot 1/2H_2O$ derivative (Scheme 1) can undergo an almost total (up to 92 % at least) isomerization to $[Ru^{II}(py)_4Cl(ON)](PF_6)_2 \cdot 1/2H_2O$ in solid state, after irradiation at 476 nm,[23] which denotes an extreme sensitivity to light for this species. As both metal nitrosyl isomerization and NO release are based on the same general concept of photo-reactivity, investigating the capabilities of $[Ru^{II}(py)_4Cl(NO)]^{2+}$ cations for NO release becomes naturally addressed. However, the stability of ruthenium pyridine complexes in biological medium would likely be limited, and therefore, $[Ru^{II}(L)_xCl_y(NO)]^{z+}$ (L = 2,2'-bipyridine; 1,10-phenantroline; 2,2':6',2''-terpyridine (terpy)) should lead to more suitable candidates for practical applications. Along this line, we have recently reported on various ruthenium-nitrosyl complexes built up from 4'-substituted terpyridines of general formula $[Ru^{II}(R-terpy)Cl_2(NO)]^+$ (Scheme 1) exhibiting potential light-sensitivity. In such systems, the photorelease of NO is ultimately related to electronic transitions having a strong charge transfer character to the nitrosyl fragment, according to the following simplified reaction (2):

$$[Ru^{II}-NO^+] \rightarrow [Ru^{III}] + NO^\bullet \qquad (2)$$
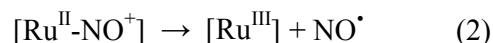
Therefore, the use of terpyridines bearing donor substituents seems especially appealing to enhance the Ru→NO charge transfer, and hence the NO release capabilities.

2

In the present paper, we report on [Ru^{II}(R-terpy)Cl$_2$(NO)]$^{1+}$ complexes built up from a 4'-(2-fluorenyl)-2,2':6',2''-terpyridine (FT in Scheme 1). Apart from its slight donating character, the selection of fluorene was motivated by its well documented capability for two-photon absorption (TPA) properties.[24-28] In the last decade, TPA has emerged as the most promising photo-dynamic therapy (PDT) technics in cancer treatment, by virtue of its low damage effects, high selectivity and deep penetration into biological tissues.[29,30] Therefore, investigating chromophores based on fluorene has become a promising approach. After the report of the synthesis, separation and characterization of the different ruthenium complexes (Scheme 1), the X-ray crystal structures of FT and *trans*(Cl,Cl)-[Ru^{II}(FT)Cl$_2$(NO)](PF$_6$) will be presented. For the first time, the comparison of the optical and photo-chemical properties between *cis*(Cl,Cl)- and *trans*(Cl,Cl)- ruthenium-nitrosyl complexes will be reported and discussed within the theoretical framework of the DFT method.

Results and discussion

Synthesis and characterization.

The 4'-(2-fluorenyl)-2,2':6',2''-terpyridine (FT) ligand was prepared with a procedure similar to that described for 9,9-bisdiethyl-fluorene-4'-terpyridine.[31] This two-step synthesis is outlined in Scheme 2. FT was obtained in good yield by applying the condensation and ring closure approach developed by Kröhnke.[32]

The synthesis of the [Ru^{II}(FT)Cl$_2$(NO)](PF$_6$) derivatives was carried out by following a procedure previously reported by Nagano *et al*. using unsubstituted terpyridine.[33] In fact, when K$_2$[RuCl$_5$(NO)] reacts with terpyridine, the authors stated that the *trans*(Cl,Cl)-[Ru^{II}(terpy)Cl$_2$(NO)](PF$_6$) isomer is obtained exclusively (yield 54%) whereas use of [RuCl$_3$(H$_2$O)$_2$(NO)] leads to *cis*(Cl,Cl)- derivative (yield 44%) according to Reedijk.[34] In the present investigation, the ^{1}H NMR spectra of the crude complex was obtained in acetonitrile solution showing the presence of three different species: *cis*(Cl,Cl)-[Ru^{II}(FT)Cl$_2$(NO)](PF$_6$), *trans*(Cl,Cl)-[Ru^{II}(FT)Cl$_2$(NO)](PF$_6$), and the homoleptic [Ru^{II}(FT)$_2$](PF$_6$)$_2$ complex (see Figure S1). Separation of the three compounds was achieved by preparative HPLC (reverse phase) by using a mixture of acidified water (1% trifluoroacetic acid) and acetonitrile (see experimental section) in various proportions to elute the complexes. The complexes eluted at retention times of 3.38, 3.58, and 4.64 min, corresponding to *cis*(Cl,Cl)-, *trans*(Cl,Cl)- and homoleptic complexes, respectively. *Cis*(Cl,Cl)- and *trans*(Cl,Cl)- geometries of the complexes were assigned by the chemical shifts of the ^{1}H signals and enabled the evaluation of the proportion of the different isomers. The ^{1}H NMR spectra in acetonitrile are shown in Figure 1, for the separated *cis*(Cl,Cl)-[Ru^{II}(FT)Cl$_2$(NO)](PF$_6$) and *trans*(Cl,Cl)-[Ru^{II}(FT)Cl$_2$(NO)](PF$_6$) derivatives. The signals of the *cis*- isomer are shifted to lower field compared to those of the *trans*- isomer as assumed by Nagao,[33] and as we have recently observed in analogous ruthenium complexes.[35] The chemical shifts of all the signals were

identified from two dimensional NMR HMBC, HSQC, long and short range COSY spectra for *cis*- and *trans*- complexes. Our assumption was confirmed by X-Ray analysis of *trans*(Cl,Cl)-[Ru^{II}(FT)Cl$_2$(NO)](PF$_6$) (*vide infra*).

The frequency of the ν(NO) stretching vibration has also been suggested to be a good indicator of the relative coordination site of the NO ligand with respect to nitrogen atoms of the terpy or the chloride ligands. Thus in the *cis*(Cl,Cl)- isomer, which involves a coordinated chloride trans to NO, ν(NO) stretching vibration is observed at 1894 cm^{-1} whereas the value increases to 1901 cm^{-1} in the *trans*(Cl,Cl)- isomer, contrary to the report of Nagao.[33] Indeed, Nagao reports ν(NO) values of 1895 cm^{-1} and 1928 cm^{-1} for the *trans*(Cl,Cl)-, and *cis*(Cl,Cl)-[Ru(terpy)Cl$_2$(NO)]$^+$ complexes, respectively (PF$_6^-$ being the counter-ion). However, and apart from these solid state data, Nagao observed similar *trans/cis* values in solution: 1903 cm^{-1} (*trans*) and 1904 cm^{-1} (*cis*). It seems therefore that, if the intrinsic ν(NO) energies fall in the same range of magnitude for both isomers, the observed differences arise largely from different solid state environments. Along this line, Reedijk[34] reports on a value of 1860 cm^{-1} for the same [Ru(terpy)Cl$_2$(NO)]$^+$ complex but with Cl$^-$ as the counter ion, which confirms the importance of solid state effect. One can infer from these observations that founding a ν(NO) value higher in the *trans* isomer than in the *cis* isomer may be possible in some case. In our compound, a DFT computation performed in acetonitrile medium leads to 2013 cm^{-1} (*trans*) and 2004 cm^{-1} (*cis*). These values confirm that ν(NO) energies are intrinsically close to each other in the two isomers, and qualitatively agree with our experimental data: 1901 cm^{-1} (*trans*(Cl,Cl)) and 1894 cm^{-1} (*cis*(Cl,Cl)).

We also have tested the influence of the concentration of KCl used in the reaction on the ratio of *cis/trans* isomers.[34,36] Using 13 equivalents of KCl leads to *cis/trans* ratio of 18/47, with 35% of homoleptic [Ru(FT)$_2$](PF$_6$)$_2$. Increasing the quantity to 21 equivalents of KCl changes faintly the value to 20/38 although the proportion of the homoleptic complex is the highest (42%). In our case, 13 equivalent of KCl was preferred to favor the formation of the desired Ru^{II}(NO) complexes. The fact that the *trans*- isomer is dominant in the *cis/trans* synthetic mixture is consistent with the DFT computation of the Gibbs free energies which indicates a stabilization of 0.40 kcal.mol^{-1} for the *trans*- isomer with respect to the related *cis*- derivative. Indeed, assuming a Boltzmann distribution at a reaction temperature around 350 K leads to a [*cis*] / [*trans*] ratio of 0.56, in the same range of the observed [*cis*] / [*trans*] value (18/47 = 0.38). Therefore, one can assume that the *cis/trans* product of the reaction is qualitatively thermodynamically controlled, to a large extent.

The spectroscopic (IR, NMR) data, the diamagnetic properties and X-Ray diffraction structure indicate that the *cis*(Cl,Cl)- and *trans*(Cl,Cl)-[Ru^{II}(FT)Cl$_2$(NO)](PF$_6$) can be described as {Ru(NO)}^{6} systems, according to Enemark-Feltham notation.[37]

Crystal structure description

4'-(2-fluorenyl)-2,2':6',2''-terpyridine (FT) crystallizes in the $Pna2_1$ orthorhombic space group, with a single molecule in the asymmetric unit cell. The molecular unit of FT is shown in Figure 2, with the atom labeling scheme. Despite 18 short contacts between neighboring molecules, the shortest being observed at 2.570 Å between N(2) and H(21), there is no π-stacking in the crystal. The terpyridine fragment is grossly planar with main deviation of 0.568 Å from the mean plane observed at H(15). As in other terpyridine systems, the nitrogen atoms are in the *trans* position to each other in order to minimize the interactions between the nitrogen lone pairs. The torsion angle between the mean plane of the fluorenyl substituent (22 atoms) and that of the terpyridine moieties (28 atoms) is equal to 30.23°. Interestingly, the corresponding DFT-computed angle is equal to 34.88°, which accounts fairly well for the weakness of intermolecular interactions in the present case.

The *trans*-[Ru^{II}(FT)Cl$_2$(NO)](PF$_6$) compound crystallizes in the P-1 triclinic space group, with a single ruthenium complex per asymmetric unit cell. The cationic *trans*-[Ru^{II}(FT)Cl$_2$(NO)]$^+$ complex is shown in Figure 3. A molecule of methanol per asymmetric unit cell, coming from the HPLC eluent, is evidenced in the structure. In contrast with the free ligand, the terpyridine is nearly planar, with largest deviation of 0.027 Å observed at H(9). The ruthenium atom lies 0.013 Å above the mean plane of the terpyridine fragment. A total of 31 short contacts (5 of them shorter than 2.5 Å) are observed per [Ru^{II}(FT)Cl$_2$(NO)]$^+$, which leads to an important set of intermolecular interactions. All the aromatic rings are roughly parallel, and the resulting structure arises from layers of chromophores roughly oriented in the YZ crystallographic plane. Owing to this important packing effect, the torsion angle between the terpyridine (28 atoms) and fluorenyl moieties (22 atoms) is reduced to 4.79°, a value, which strongly contrasts with the DFT-computed angle of 34.19°. An additional DFT computation performed on a complex baring a planar fluorenylterpyridine ligand indicates that the resulting conformation is destabilized by 2.18 kcal/mol. This indicates that the torsion angles between fluorenyl and terpyridine moieties are energetically relevant, and therefore supports the idea that the solid state conformation is largely influenced by intermolecular interactions for this ruthenium complex. Crystal data for the two X-ray structures are gathered in Table 1. Despite several attempts, no suitable single crystals were obtained for the *cis*-derivative.

Optical spectra

The UV-visible spectra of fluorenylterpyridine (FT), *trans*- and *cis*-[Ru^{II}(FT)Cl$_2$(NO)](PF$_6$), recorded in acetonitrile, are shown in Figure 4. The spectrum of the ligand is built up from a single band located in the 275-350 nm domain, arising from two main components (λ_{max} at 297 nm and 309 nm), and exhibits an extinction coefficient (ε) of 30 800 mol^{-1}.L.cm^{-1}. In contrast, the spectra of the two ruthenium complexes appear much more complicated, with main features summarized as follows: (*i*) an intense band (A) around 280 nm nearly identical for the two *cis*- and *trans*- isomers; (*ii*) a second and low-lying band (B) located around 400 nm, slightly blue-shifted in the *cis*-isomer; (iii) additional transitions of lower intensities are

5

present as shoulders between bands A and B. While band A seems to be reminiscent of that of the ligand, the appearance of a band at 400 nm suggests that the ruthenium-nitrosyl fragment has a dominant contribution at this wavelength, and encouraged further photolysis experiments. The main spectroscopic data are gathered in Table 2.

NO release in *cis*- and *trans*-[Ru^{II}(FT)Cl$_2$(NO)](PF$_6$).

The photoactivity of ruthenium-nitrosyls has been known for over 40 years, and was recently summarized by Mascharak.[11c] The resulting rapid release of nitric oxide (as evidenced by response of an NO-sensitive sensor) is followed by the formation of a solvent bound ruthenium(III) photoproduct, according to the following equation:

$$(L)Ru^{II}\text{-}NO + solvent \xrightarrow{h\nu} (L)Ru^{III}\text{-}solvent + NO^{\bullet} \quad (3)$$
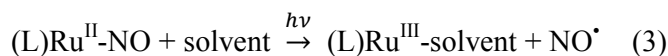
This reaction can be followed spectroscopically by the appearance of a broad and low-lying electronic transition ascribable to a ligand $\rightarrow$ Ru^{III} charge transfer, largely red shifted with respect to the related ligand $\rightarrow$ Ru^{II} charge transfer. Additionally, the close-shell (d^6) Ru^{II} is replaced by the paramagnetic Ru^{III} ion, the presence of which can be targeted by electrochemistry and electron paramagnetic resonance (EPR) spectroscopy.

The changes in the electronic absorption spectra of *trans*- and *cis*-[Ru^{II}(FT)Cl$_2$(NO)](PF$_6$) exposed to 405 nm light in acetonitrile are shown in Figure 5. For both isomers, the presence of isosbestic points at 286, 366, and 428 nm (*cis*(Cl,Cl) isomer) and at 284, 376, and 468 nm (*trans*(Cl,Cl) isomer) indicates a clean conversion of the Ru^{II}(NO) complexes to related photolysed species. It is important to note that no back-reaction is observed when the light is turned off. In the photolysed *cis*(Cl,Cl) species, new bands located at 350, 400 – 450, and 600 – 630 nm arise. In the *trans*(Cl,Cl) species, equivalent increasing bands at 350, and 600 – 630 nm are observed. Interestingly, a new and large band at 400 – 450 nm is also present in the *trans*(Cl,Cl) photolysed species. However, this band of weak intensity is largely hidden by the intense band at 414 nm present in the starting *trans*-[Ru^{II}(FT)Cl$_2$(NO)](PF$_6$), in such a way that it is difficult to state whether this transition is appearing or not during the photolysis process. Nevertheless, it is interesting to observe that the final photolysed species exhibit closely related UV-visible spectra arising either from the *cis*- or *trans*- starting derivatives.

The quantum yields observed for NO release from *trans*- and *cis*-[Ru^{II}(FT)Cl$_2$(NO)](PF$_6$) at 405 nm light irradiation are 0.106 and 0.307 respectively. These values are surprisingly different and are in the range of quite high NO quantum yields values for ruthenium nitrosyl complexes. They lie in the same order of magnitude of similar terpyridine-Ru(NO) complexes studied by da Silva *et al.*, in which values of 0.14, 0.46, and 0.47 have been reported for [Ru(L)terpy(NO)]$^{3+}$ (L = 2,2'bipyridine, quinone-diimine, *o*-phenylenediamine, respectively).[38]

Additional experiments have been carried out to confirm that the photoreaction corresponds to that of equation 3. The NO release upon irradiation was verified by the Griess test which involves an *in situ* oxidation of the released NO to NO_2^- in aqueous medium, under aerobic condition, followed by a reaction with sulfanilic acid, thus providing a diazonium cation, and finally the formation of a pink azo dye (λ_{max} = 548 nm).[39] The changes observed in the optical spectrum of *cis*-[Ru^{II}(FT)Cl$_2$(NO)](PF$_6$) irradiated at 405 nm in the presence of the Griess reagent are shown in Figure 6. The gradual appearance of a pink color is clearly evidenced from the experimental data, and undoubtedly proves that NO release takes place under irradiation. It is important to point out that, without irradiation, no color change is evidenced, which indicates the chemical stability of the Ru^{II}(NO) complexes. Both *cis*- and *trans*-isomers exhibit the same qualitative behavior, once submitted to the Griess test. Moreover, the appearance of a broad low-energy band in the 600 – 630 nm range arising from π-conjugated ligand to ruthenium(III) charge transfer transition after NO photo-release is well documented.[40-42] Additional experimental support should be found from EPR. However, we have observed no signal in the X-band EPR spectrum on an irradiated sample of *trans*-[Ru^{II}(FT)Cl$_2$(NO)](PF$_6$), contrary to the report of paramagnetic ruthenium(III) highlighted by Mascharak after photolysis of ruthenium(II)-nitrosyl complexes.[40] This unexpected behavior has occasionally been observed in Ru^{3+} ions, which may be EPR silent due to fast electron spin relaxation, in some cases, even at low temperature.[43,44]

More convincing experimental features are available from electrochemistry. The cyclic voltammograms have been recorded for the *cis*/*trans*- Ru^{II}(NO) species and for their related photolysed product. The results are gathered in Table 3. The *trans*-Ru^{II}(NO) complex exhibits two reduction waves at -0.13 V and -0.62 V (*vs* SCE), which are respectively ascribed to a Ru^{II}NO$^+$ → Ru^{II}NO$^•$ and Ru^{II}NO$^•$ → Ru^{II}NO$^-$ reduction, according to previous reports on polypyridine Ru^{II}(NO) systems.[45,46] The first redox process (-0.13 V) is reversible at a scan rate of 10 V/sec, but becomes gradually irreversible when the scan rate is reduced to lower values. Furthermore, the complexes are oxidized irreversibly at + 1.85 V and + 2.4 V. The first oxidation couple is an irreversible process observed in the [Ru^{II}(FT)$_2$](PF$_6$)$_2$ and FT reference species as well, and is therefore attributed to the oxidation of the ligand. The second one (+ 2.4 V) cannot be determine very precisely as it falls at the upper limit of the electrochemical window of the solvent. Nevertheless, it corresponds to the Ru^{III} / Ru^{II} redox couple, which has been found to be switched to very high potential in related species due to the strong withdrawing effect of ligand NO$^+$ ligand.[45-47] The voltammograms of the photolysed complexes appear deeply modified by irradiation at 405 nm, with three main features summarized as follows: (i) the waves ascribed to the reduction of NO$^+$ into NO$^•$ and NO$^-$ are absent, which indicates complete NO release after irradiation ; (ii) the oxidation of the FT ligand observed at 1.85 V remains grossly unaffected after NO release. This behavior is consistent with the computational analysis of the HOMO level in these complexes (*vide infra*). Indeed, the electron density is fully localized on the fluorenyl fragment at the HOMO level, far away from the Ru(NO) core. Therefore, and to a large extent, we may infer that the release of the NO$^•$ radical will have a very modest influence on the HOMO of the ruthenium complex, and hence on its oxidation potential. Finally (iii) the Ru^{II} → Ru^{III} oxidation wave at ~2.4 V in the starting complexes is replaced by a fully reversible reduction wave observed at

7

0.45 V, in a range of potential typical of that of a reduction of Ru^{III} into Ru^{II} species free of NO^+,[47] These modifications strongly support the appearance of Ru^{III} species after irradiation of the *trans*-Ru^{II}(NO) compound, as anticipated from equation 3. The same general features are observed in the *cis*-Ru^{II}(NO) complex, with main differences from the parent *trans*-isomer being observed in the reduction behavior. Indeed, an easier reduction of NO^+ into $NO^•$ (50 mV) is clearly observed in the case of the *cis*- derivative. This difference may tentatively be related to the fastest NO release observed, during which NO acts as an oxidant.

DFT analysis

The experimental and DFT computed data are gathered in Table 2. There is a general trend for a blue-shift of about 30-40 nm in the calculated wavelength, with respect to the experimental data, which falls in the widely accepted range of TD-DFT uncertainty (0.3 – 0.5 eV). The agreement between theory and experiment appears satisfactory, with the presence of two main transitions, and shoulders in-between, and a slight blue-shift of 15 nm in the band B of the *cis*-derivative with respect to the *trans*- related complex.

The main features of the low-lying band (B) of the Ru^{II}(NO) complexes are gathered in Table 4, with that of FT ligand. It clearly appears from the data, that these bands arise from a single transition having a dominant HOMO → LUMO character. These orbitals are drawn in Figure 7, for *cis*- and *trans*-$[Ru^{II}(FT)Cl_2(NO)]^+$. From their careful examination, the electronic features of the related transitions can be summarized as follows: (i) the transitions bring electrons in orbitals exhibiting a strong antibonding character between ruthenium and nitrosyl fragments, thus leading to a weakening of the Ru-NO bond, and hence a potential for NO release; (ii) the resulting observed charge transfers correspond to an oxidation of the complexes by the nitrosyl ligand, which is assumed to be present as NO^+ in the complex and as $NO^•$ after breaking of the Ru-NO bond. Consequently the DFT description of the low-lying transitions present in both *cis*- and *trans*-$[Ru^{II}(FT)Cl_2(NO)]^+$ provides a rationale for the experimental observation of NO release after irradiation at 405 nm.

The origin of the significant difference observed in the quantum yield of the photo-dissociation for both *cis*(Cl,Cl)- and *trans*(Cl,Cl)- isomers (0.307 and 0.106, respectively) has been tentatively targeted computationally. DFT optimizations conducted at the ground state and at the 6th excited state (1 → 7 transition) lead to the appearance of the following modifications on the Ru-NO fragment upon irradiation: (*i*) elongation of the Ru-NO bond of about 0.1 Å and (*ii*) binding of the linear Ru-NO to an angular value around 145°. These changes evidenced for both *cis/trans* isomers are detailed in Table 5. Increase of ruthenium-nitrogen bonds clearly indicates a weakening of the Ru-NO bond, while a binding coordination is consistent with the occurrence of a significant Ru^{II} to NO^+ charge transfer, as previously reported,[37] leading to a charge localization close to that observed in the dissociated species: $[Ru^{III}(FT)Cl_2]^+$ and $NO^•$. Interestingly, both effects which favor the NO release are more pronounced in the *cis*(Cl,Cl)- derivative, in qualitative agreement with the experimental observation of a faster photoreactivity in this isomer.

Additional insights about the weakening of the ruthenium-nitrogen bond may be found from the careful examination of the main orbital involved in the intense $1 \rightarrow 7$ transitions of the complexes. While the HOMO level does not imply any ruthenium and nitrosyl contributions, the Ru-NO overlap is important, and nonbonding, at the LUMO level. The atomic coefficients are provided in Table 5, showing a higher electron density present between Ru and N in the *cis*- derivative and therefore a qualitative trend for a more pronounced antibonding character, and hence an increased tendency for bond-order reduction upon irradiation.

Finally, the role devoted to the fluorene substituent was addressed from a computational study of *trans*(Cl,Cl)-[Ru^{II}(FT)Cl$_2$(NO)]$^+$ compared to that of the parent *trans*(Cl,Cl)-[Ru^{II}(terpy)Cl$_2$(NO)]$^+$ (terpy = 2,2':6',2''-terpyridine). While *trans*(Cl,Cl)-[Ru^{II}(FT)Cl$_2$(NO)]$^+$ exhibits an intense transition calculated at 370 nm arising from an intense intramolecular (fluorene $\rightarrow$ nitrosyl) charge transfer, the corresponding charge transfer has a reduced magnitude in the complex built up from the unsubstituted terpyridine, and leads to a band shifted to 326 nm. Such a red-shift obtained from an extension of conjugation in the in-plane ligand frame has been previously pointed out by Mascharak on polydentate N-ligands.[40] With experimental λ_{max} of 414 and 389 nm for the *trans*- and *cis*- complexes, respectively, the present species seem to offer no practical interest because they fall out of the 600-1 300 nm range of therapeutic window[48] defined as the spectroscopic domain outside the region were light is greatly absorbed by hemoglobin or melanin ($\lambda < 600$ nm) and by tissue water ($\lambda > 1\,300$ nm). Nevertheless, fluorene-based chromophores frequently exhibit TPA properties. Along this line, λ_{max} around 400 nm and quantum yield of photo-release in the 0.1-0.3 range make them potential candidate for PDT technics with irradiation around 800 nm.

Experimental

Materials and equipment

1-(2-oxo-2-pyridin-2-yl-ethyl)pyridinium iodide[49] and K$_2$[RuCl$_5$NO][50] were prepared according to literature protocols. The Griess reagent used for the NO detection was obtained from Sigma.

2-acetylpyridine and fluorene-2-carboxaldehyde were obtained from Alfa-Aesar; the solvents were analytical grade and used without further purification. Elemental analyses were performed at LCC with a Perkin Elmer 2400 serie II Instrument. ^{1}H and ^{13}C NMR spectra were obtained at 298K in CDCl$_3$, CD$_3$CN or (CD$_3$)$_2$SO as internal reference and were recorded on a Bruker Avance 400 and or for 2D NMR on a Bruker Avance 500. *J* values are given in Hertz. Infrared spectra were recorded on a Perkin Elmer Spectrum 100 FT-IR Spectrometer, using a diamond ATR.

Electrospray Ionization Mass Spectroscopy was carried out on a XevoG2QTof spectrometer and on a QTRAP 2000 spectrometer coupled with UPLC Aquity chain (Waters SA).

Separation of the complexes was achieved by preparative HPLC on Acquity chain (Waters SA) with UV-Vis detector diode array (200-800nm). The used column is Acquity BEH C18 50 mm × 2.1 mm (inverse phase). Elution was carried out with a mixture of water acidified with 1% of trifluoroacetic acid and methanol, in variable proportions with time.

Synthesis

4'-(2-fluorenyl)-2,2':6',2''-terpyridine (FT). To a methanolic suspension (9 mL) of fluorene-2-carboxaldehyde (1.164 g, 6 mmol) and 2-acetylpyridine (0.74 mL, 6 mmol) cooled at 0°C was added dropwise aqueous NaOH (6 mL, 1 M). The mixture was brought to room temperature and stirred for 2 hours. The crude pale yellow product formed was filtered, rinsed with cool MeOH (1.511 g was obtained) and purified by column chromatography on Alumina (eluant: AcOEt/CH$_2$Cl$_2$ 1/9), and yielded 0.9 g (50%) for **1** (Scheme 2). Elemental analysis found: C, 84.82; H, 4.56; N, 4.53 %. C$_{28}$H$_{19}$N$_3$ requires C, 84.82; H, 5.08; N 4.71 %. **^{1}H NMR (CDCl$_3$, 400 MHz)**: δ 8.82 (d, ^3J 4, 1H), 8.42 (d, ^3J 15.9, 1H), 8.28 (d, ^3J 7.7 , 1H), 8.08 (d, ^3J 15.9, 1H), 8.00 (s, 1H), 7.97 (td, ^3J 7.7, ^4J 1.7, 1H), 7.85 (d, ^3J 7.7, 2H), 7.81 (t, ^3J 7.4, 1H), 7.60-7.57 (m, 2H), 7.41 (t, ^3J 7 , 1H), 7.37 (td, ^3J 7.4, ^4J 1.3, 1H), 3.98 (s, 2H).

A mixture of **1** (445mg, 1.5mmol), 1-(2-oxo-2-pyridin-2-yl-ethyl)pyridinium iodide (489 mg, 1.5 mmol) and ammonium acetate (1.5 g, 19.5 mmol) and ethanol (6 mL) were refluxed for 12 h. The resulting precipitate was collected by filtration, rinsed with cold EtOH, water and dried. Yield for **2** (546 mg, 91%). Elemental analysis found: C, 84.25; H, 4.23; N, 10.47 %. C$_{28}$H$_{19}$N$_3$ requires C, 84.61; H, 4.82; N, 10.57%. **^{1}H-NMR (CDCl$_3$, 400 MHz)**: δ (ppm) 8.80 (2H, s, H-3'and 5'), 8.75 (2H, ddd, ^3J 4.8, ^4J 1.7, ^5J 0.8, H-6 and 6''), 8.71 – 8.67 (2H, m, H-3 and 3''), 8.11 (1H , s, H-1f), 7.94 (1H, dd, ^3J 8.0, ^4J 1.6 Hz, H-3f), 7.91 (1H , br s, H-4f), 7.89 (2H, td, ^3J 7.8, ^4J 1.9, H-4 and 4''), 7.86 (1H, d, ^3J 7.5 , H-5f), 7.60 (1H, d, ^3J 7.4 , H-8f), 7.42 (1H, td, ^3J 7.2, ^4J 0.7 , H-7f), 7.40 – 7.34 (2H, m, H-5 and 5''), 7.36 – 7.32 (1H, m, H-6f), 4.01 (2H, s, H-9f). **^{13}C-NMR (CD$_3$CN, 125 MHz)**: δ (ppm) 156.36 (C-2 and 2''), 155.90 (C-4'), 150.55 (C-2' and 6'), 149.14 (C-6 and 6''), 143.98 (C-11f), 143.75 (C-10f), 144.63 (C-13f), 141.16 (C-12f), 136.93 (C-4 and 4''), 136.87 (C-2f), 127.14 (C-6f), 126.90 (C-7f), 126.23 (C-3f), 125.15 (C-8f), 123.96 (C-1f), 123.81 (C-5 and 5''), 121.40 (C-3 and 3''), 120.26 (s, C-4f/C-5f), 120.24 (s, C-5f/C-4f), 118.81 (C-3' and 5'), 36.98 (C-9f).

Ruthenium complexes. A mixture of K$_2$[RuCl$_5$(NO)] (175 mg, 0.45 mmol), ligand FT (180 mg, 0.45 mmol) and KCl (438 mg, 5.88 mmol) in aqueous ethanol (35 mL, 3 parts of EtOH for 1 part H$_2$O) was refluxed for one hour. After cooling down, a grey precipitate with some black parts was filtered off and two equivalents of NH$_4$PF$_6$ in concentrated aqueous solution were added in the filtrate. The reddish precipitate obtained was filtered on a büchner, washed with water and dried. The total weight is 120 mg. ^{1}H NMR showed the presence of three compounds which were separated by HPLC:

Trans(Cl,Cl)-[Ru^{II}(FT)Cl$_2$(NO)](PF$_6$). Yield of isolated compound 30 mg, 9%. **^{1}H-NMR (CD$_3$CN, 500 MHz)**: δ (ppm) 8.80 (2H, s, H- 3'and 5'), 8.78 (2H, dd, ^3J 5.6, ^4J 0.8, H-6 and

6''), 8.70 (2H, d, ^3J 8.0, H-3 and 3''), 8.39 (2H ,td, ^3J 7.8 ^4J 1.3 , H-4 and 4''), 8.32 (1H , s, H-1f), 8.14 (1H, d, ^3J 8.1 , H-4f), 8.13 (1H, d, ^3J 8.1 , H-3f), 8.01 (1H, d, ^3J 7.1, H-5f), 7.88 (2H, ddd, ^3J 7.8, ^3J 5.6, ^4J 1.3 , 5 and 5''-H), 7.69 (1H, d, ^3J 7.2 , H-8f), 7.51-7.47 (1H, m , H-6f), 7.46 (1H, td, ^3J 7.4, ^4J 1.2 , H-7f), 4.11 (2H, s, H-9f). **^{13}C-RMN (CD$_3$CN, 125 MHz)**: δ (ppm) 155.75 (C-2 and 2''), 157.32 (C-4'), 153.67 (C-2' and 6'), 154.66 (C-6 and 6''), 146.33 (C-11f), 149.35 (C-10f), 145.22 (C-13f), 143.02 (C4 and 4''), 140.98 (C-12f), 133.75 (C-2f), 130.57 (C-5 and 5''), 128.94 (C-7f), 127.80 (C-6f), 127.19 (C-3 and 3''), 126.01 (C-8f), 125.71 (C-1f), 123.15 (C-3' and 5'), 143.02 (C-4f), 121.61 (C-5f), 128.04 (C-3f), 37.29 (C-9f). IR(KBr): ν_{max}(cm^{-1}) 1901(N-O). Mass (ESI): m/z 599.30 for [M]$^+$. Elemental analysis found: C,43.10 ; H,2.23 ; N, 6.19 %. C$_{28}$H$_{19}$N$_4$ORuCl$_2$PF$_6$ ·2 H$_2$O requires C, 43.09 ; H,2.97 ; N 7.18 %.

Cis(Cl,Cl)-[Ru^{II}(FT)Cl$_2$(NO)](PF$_6$). Yield of isolated compound 10mg, 3%. **^{1}H-NMR (CD$_3$CN, 500 MHz)**: δ (ppm) 9.20 (2H, dd, ^3J 5.5, ^4J 1.2 ,H-6 and 6''), 8.96(2H, s, H-3'and 5'), 8.81 (2H, d, ^3J 7.9, H-3 and 3''), 8.47(2H ,td, ^3J 7.9, ^4J 1.3 , H-4 and 4''), 8.45(1H , s, H-1f), 8.21(1H, d, ^3J 8.0, H-3f), 8.17(1H, d, ^3J 8.0 , H-4f), 8.01(1H, d, ^3J 7.3 , H-5f), 7.98-7.93(2H, m, H-5 and 5''), 7.69 (1H, d, ^3J 7.3, H-8f), 7.51-7.47 (1H, m, H-6f), 7.45 (1H, td, ^3J 7.4 ^4J 1.3, H-7f), 4.14 (2H, s, H-9f). **^{13}C-RMN (CD$_3$CN, 125 MHz)**: δ (ppm) 157.65 (C-2 and 2''), 156.43 (C-4'), 153.69 (C-2' and 6'), 153.22 (C-6 and 6''), 145.32 (C-11f), 145.02 (C-10f), 144.63 (C-13f), 142.78 (C4 and 4''), 140.19 (C-12f), 133.36 (C-2f), 129.43 (C-5 and 5''), 128.32 (C-7f), 127.24 (C-f6), 126.53 (C-3 and 3''), 125.46 (C-8f), 125.22 (C-1f), 122.91 (C-3' and 5'), 121.06 (C-4f), 121.02 (C-5f), 117.47 (C-3f), 36.75 (C-9f). IR(KBr): ν_{max}(cm^{-1}) 1894(N-O). Mass (ESI): m/z 599.20 for [M]$^+$.

[Ru^{II}(FT)$_2$](PF$_6$)$_2$. Yield of isolated compound 50 mg, 9% **^{1}H-NMR (CD$_3$CN, 500 MHz):** δ (ppm) 9.12 (2H, s, H-3'and 5'), 8.71 (2H, d, ^3J 8.0, H-3 and 3''), 8.49 (1H , s, H-1f), 8.30 (1H, dd, ^3J 7.9, ^4J 1.6, H-3f), 8.25 (1H, d, ^3J 7.9, H-4f), 8.07 (1H, d, ^3J 7.4, H-5f), 7.99 (2H ,td, ^3J 7.9, ^4J 1.4 , H-4 and 4''), 7.76 (1H, d, ^3J 7.3, H-8f), 7.55 (1H, t, ^3J 7.3, H-6f), 7.52 -7.46 (3H, m, H-6, 6''and H-7f), 7.23 (2H, ^3J 7.1, ^3J 5.7, ^4J 1.2 , ddd, H-5 and 5''), 4.23 (2H, s, H-9f). **^{13}C-RMN (CD$_3$CN, 125 MHz) :** δ (ppm) 158.30 (C-2 and 2''), 155.44 (C-2' and 6'), 152.48 (C-6 and 6''), 148.49 (C-4'), 145.00 (C-10f), 144.35 (C-13f), 143.85 (C-11f), 140.56 (C-12f), 138.04 (C4 and 4''), 135.10 (C-2f), 127.92 (C-7f), 127.44 (C-5 and 5''), 127.19 (C-6f), 126.72 (C-3f), 125.45 (C-8f), 124.53 (C-3 and 3'' or C-1f), 124.49 (C-1f or C-3 and 3''), 121.45 (C-3' and 5'), 120.97 (C-4f), 120.72 (C-5f), 36.81 (C-9f). Mass (ESI): m/z 448.11 for [M]$^{2+}$ and m/z 1041.18 for [M-PF$_6$]$^+$. Elemental analysis found: C, 56.53 ; H, 3.07 ; N, 6.83 %. C$_{56}$H$_{38}$N$_6$RuP$_2$F$_{12}$ requires C, 56.71 ; H,3.23 ; N 7.09 %.

Crystallographic studies

Single crystals of FT were obtained by slow evaporation of a concentrated solution in acetone. Single crystals of *trans*-[Ru^{II}(FT)Cl$_2$(NO)](PF$_6$) were grown by slow diffusion of Et$_2$O into a concentrated solution of the complex in acetonitrile.

11

Diffraction data were collected at low temperature (180 K) on a Bruker Kappa Apex II diffractometer, using a graphite-monochromated source or a 30 W air-cooled microfocus source and focusing multilayer optics, with MoKα radiation (λ = 0.71073 Å). The diffractometer is equipped with an Oxford Cryosystems Cryostream cooler device. The structures were solved by direct methods with SHELXS-97. All non-hydrogen atoms were refined anisotropically by means of least-squares procedures on F² with the aid of the program SHELXL-97.[51] The H atoms were refined isotropically at calculated positions using a riding model with their isotropic displacement parameters constrained to be equal to 1.5 times the equivalent isotropic displacement parameters of their pivot atoms for terminal sp^3 carbon or hydroxyl group and 1.2 times for all other carbon atoms. The disordered solvent molecule (MeOH) in *trans*-[Ru^{II}(FT)Cl$_2$(NO)](PF$_6$) was modelled successfully. The atom ellipsoids were restrained by using SIMU and DELU commands.

The two crystal structures have been deposited with the Cambridge Crystallographic Data center (CCDC 994941 and 994942, for FT and *trans*-[Ru^{II}(FT)Cl$_2$(NO)](PF$_6$), respectively).

DFT computations

The two ruthenium complexes (*trans*(Cl,Cl)- and *cis*(Cl,Cl)-[Ru^{II}(FT)Cl$_2$(NO)](PF$_6$)) and the related fluorenylterpyridine were fully optimized using the Gaussian-09 program package[52] within the framework of the Density Functional Theory (DFT). In any case, the calculations were performed in the presence of acetonitrile, which was modelized by the Polarizable Continuum Model (SCRF=PCM method).[53] The double-ζ basis set 6-31G* was used for all atoms except the heavy ruthenium atom, for which the LANL2DZ basis set was applied to account for relativistic effects.[54] Following the previous report on ruthenium-nitrosyl by Mascharak,[55] we have selected the hybrid functional B3PW91 for the optimization, which has been shown to outperform other hybrid functionals (*e.g.* B3LYP) and pure functionals (*e.g.* PW91) in numerous cases of ruthenium complexes,[56] especially when back bonding ligands (like NO) are present.[57] Several functionals were tested for the calculations of the UV-visible spectra (B3PW91, B3LYP, PBE0, and CAM-B3LYP) by time-dependent (TD)-DFT. CAM-B3LY[58] was finally selected, for its better accuracy to reproduce the experimental transition energies (< 0.5 eV in any case). The computed geometries of FT, *cis*- and *trans*-[Ru^{II}(FT)Cl$_2$(NO)]$^+$ are provided as Supplementary Information with the related UV-visible computed spectra.

Photochemistry

The UV-visible spectra were recorded on 3 mL of non-deoxygenated solutions of the nitrosyl complexes (0.03 mmol/L) in acetonitrile, under irradiation realized with a Muller reactor device equipped with a cooling water filter and a mercury arc lamp equipped with appropriate interference filter to isolate the desired irradiation wavelength (λ$_{max}$ = 405 nm, intensity 9 mW). The light intensity was determined by using ferrioxalate actinometer.[59] The sample solutions were placed in a quartz cuvette of 1 cm path -length stirred continuously. The

temperature was maintained at 27°C during the whole experiment. The irradiation was performed with an optical fiber fixed on the top of the cuvette and upon 40 mn. The UV-visible spectra were recorded every 10 seconds in fast scan mode during a period of 10 mn, which allows reaching apparent stable absorption conditions. Nevertheless, the irradiation was kept for 40 mn for both *cis*(Cl,Cl)- and *trans*(Cl,Cl)- ruthenium-nitrosyl complexes.

Kinetic studies on the photolysis reactions were carried out with a diode array Hewlett Packart 8454A spectrophotometer. Solutions of *trans*- and *cis*-[Ru^{II}(FT)Cl$_2$(NO)](PF$_6$) (3.10^{-5} mol.L^{-1}) in acetonitrile were used. The optical fiber was fixed at the top of the cuvette. Absorption spectra were taken after each 10 seconds.

Quantum yield measurements: Light intensities were determined before each photolysis experiments by chemical actinometry procedure. The actinometers used were potassium ferrioxalate to λ_{irr}=405 nm (I$_0$= 1.15 10^{-6} mol.L^{-1}.s^{-1}). The quantum yield (ϕ_A) was determined by the program Sa3.3 written by D. Lavabre and V. Pimienta.[60] It allows the resolution of the differential equation $\frac{d[A]}{dt} = -\Phi_A I_a^A = -\Phi_A Abs_A^\lambda I_0 F$ where I_a^A is the intensity of the light absorbed by the precursor; F, the photokinetic factor $\left(F = \frac{\left(1-10^{-Abs_{Tot}^\lambda}\right)}{Abs_{Tot}^\lambda} \right)$; Abs_A^λ , the absorbance of *trans/cis*(Cl,Cl)-[Ru^{II}(FT)Cl$_2$(NO)]$^+$ before irradiation; Abs_{Tot}^λ, the total absorbance; I$_0$, the incident intensity measured at 405nm. The equation was fitted with the experimental data $Abs_{Tot}^\lambda = f(t)$ and 2 parameters ϕ_A and ε_B (ε_B is the molar extinction coefficient measured at the end of the reaction) at two wavelengths (λ_{irr}=405 nm, λ_{obs}=354 nm). λ_{obs}=354 nm was chosen because it corresponds to a large difference between molar extinction coefficient at the initial and final time of the photochemical reaction. Simulation and optimization procedures were performed by using numerical integration and a non-linear minimization algorithm for the fitting of the model to the experimental data. [60,61]

Trans-(Cl,Cl)-[Ru^{II}(FT)Cl$_2$(NO)]$^+$
$[A]_0 = 3.01\ 10^{-5}$ mol. L^{-1}, $\varepsilon_A^{405} = 21952$ mol^{-1}. L. cm^{-1}, $\varepsilon_A^{354} = 15699$ mol^{-1}. L. cm^{-1} ,
$\varepsilon_B^{405} = 12050$ mol^{-1}. L. cm^{-1} , $\varepsilon_B^{354} = 25003$ mol^{-1}. L. cm^{-1}

Cis-(Cl,Cl)-[Ru^{II}(FT)Cl$_2$(NO)]$^+$
$[A]_0 = 2.98\ 10^{-5}$ mol. L^{-1}, $\varepsilon_A^{405} = 20305$ mol^{-1}. L. cm^{-1} ,
$\varepsilon_A^{354} = 18553$ mol^{-1}. L. cm^{-1} , $\varepsilon_B^{405} = 11847$ mol^{-1}. L. cm^{-1} , $\varepsilon_B^{354} = 25117$ mol^{-1}. L. cm^{-1}

Griess test

The Griess reagent (10 g) was dissolved in 250 mL of distilled water. Equal volume of this solution and a solution of the desired complex in acetonitrile (10^{-5} mol.L^{-1}) were irradiated at 405 nm (intensity 9 mW). UV-visible spectra were recorded each 10 seconds. The absorbance at 548 nm owing to the formation of azo dye was measured, to prove the formation of NO.

Electrochemistry

Electrochemical experiments were performed at room temperature in a homemade airtight three-electrode cell connected to a vacuum/argon line. The reference electrode was a saturated calomel electrode (SCE) separated from the solution by a bridge compartment. The counter electrode was a platinum wire of *ca.* 1 cm^2 apparent surface. The working electrode was a Pt microdisk (radius = 0.25 mm). The supporting electrolyte (nBu$_4$N)(PF$_6$) (Fluka, 99% electrochemical grade) was used as received and simply degassed under argon. Acetonitrile was freshly purified prior to use. The solutions used during the electrochemical studies were typically 10^{-3} mol.L^{-1} and 10^{-4} mol.L^{-1} respectively in *trans* and *cis* complex compound and 10^{-1} mol.L^{-1} in supporting electrolyte. Before each measurement, the solutions were degassed by bubbling argon through them, and the working electrode was polished with a polishing machine (Presi P230).

Conclusion

We have reported on the synthesis and characterization of *cis*(Cl,Cl)- and *trans*(Cl,Cl)-[Ru^{II}(FT)Cl$_2$(NO)](PF$_6$) complexes. We could show that both of them release NO under irradiation at 405 nm, with different yields. A direct comparison of the properties of these two geometrical isomers has been described, for the first time. These results reveal that geometrical tuning enables accurate modification of the NO release properties. Therefore these compounds may be regarded as potential candidates in the treatment of cancer by mean of PDT, in which the desired drug (NO) is delivered upon irradiation. Moreover, they are built up from a ligand including the fluorenyl substituent, which has widely been applied to bring about molecules with additional TPA properties. This would lead to a possible NO delivery upon irradiation around 800 nm, in a frequency range that falls in the therapeutic window. We are therefore conducting investigations of these ruthenium-nitrosyl derivatives in two directions: the determination of their TPA cross-sections and the investigation of their actions on cells cultures under irradiation.

Acknowledgements

Supplementary material

^{1}H-NMR spectrum of the mixture of isomers, DFT computed coordinated for FT, *trans*(Cl,Cl)-[Ru[II](FT)Cl$_2$(NO)][+], *cis*(Cl,Cl)-[Ru[II](FT)Cl$_2$(NO)][+], and trans(Cl,Cl)-[Ru(terpyridine)Cl$_2$(NO)][+], computed UV-visible spectra for FT, *trans*(Cl,Cl)-[Ru[II](FT)Cl$_2$(NO)][+], *cis*(Cl,Cl)-[Ru[II](FT)Cl$_2$(NO)][+], voltamograms of *trans*(Cl,Cl)-[Ru[II](FT)Cl$_2$(NO)](PF$_6$) (starting compound and photolized product).

References

1   *Nitric Oxide: Biology and Pathology*, L. J. Ignarro Ed.; Academic Press: San Diego, CA, 2000.

2   *Nitric Oxide and Cancer: Prognosis, Prevention and Therapy*, B. Bonavida Ed.; Springer 2010.

3   C. S. Degoute, *Drugs* 2007, **67**, 1053-1076.

4   *Nitric Oxide Free Radicals in Peripheral Neurotransmission*; S. Birkhauser Kalsner, Ed.; Boston, 2000.

5   J. R. Kanwar, R. K. Kanwar, H. Burrow and S. Baratchi, *Curr. Med. Chem.* 2009, **16**, 2373-2394.

6   D. Hirst and T. Robson, *J. Pharm. Pharmacol.* 2007, **59**, 3-13.

7   W. Xu, L. Z. Liu, M. Loizidou, M. Ahmed and I. G. Charles, *Cell Res.* 2002, **12**, 311-320.

8   (a) P. C. Ford, J. Bourassa, K. Miranda, B. Lee, I. Lorkovic, S. Boggs, S. Kudo and L. Laverman, *Coord. Chem. Rev.* 1998, **171**, 185-202; (b) A. K. Patra, R. K. Afshar, M. M. Olmstead and P. K. Mascharak, *Angew. Chem., Int. Ed.* 2002, **41**, 2512-2515; (c) A. K. Patra, J. M. Rowland, D. S. Marlin, E. Bill, M. M Olmstead and P. K. Mascharak, *Inorg. Chem.* 2003, **42**, 6812-6823; (d) A. A. Eroy-Reveles, C. G. Hoffman-Luca and P. K. Mascharak, *Dalton Trans.* 2007, 5268-5274.

9   (a) K. S. Suslick and R. A. Watson, *Inorg. Chem.* 1991, **30**, 912-919; (b) K. J. Franz and S. J. Lippard, *Inorg. Chem.* 2000, **39**, 3722-3733; (c) K. Ghosh, A. A. Eroy-Reveles, T. R. Holman, M. M. Olmstead and P. K. Mascharak, *Inorg. Chem.* 2004, **43**, 2988-2997; (d) C. G. Hoffman-Luca, A. A. Eroy-Reveles, J. Alvarenga and P. K. Mascharak, *Inorg. Chem.* 2009, **48**, 9104-9111.

10 (a) M. Fischer and F. Warneck, *J. Phys. Chem.* 1996, **100**, 18749-18756; (b) M. A. De Leo and P. C. Ford, *Coord. Chem. Rev.* 2000, **208**, 47-59 ; (c) F. De Rosa, X. Bu and P. C. Ford, *Inorg. Chem.* 2005, **44**, 4157-4165.

11 (a) P. C. Ford and S. Wecksler, *Coord. Chem. Rev.* 2005, **249**, 1382-1395; (b) M. J. Rose and P. K. Mascharak, *Coord. Chem. Rev.* 2008, **252**, 2093-2114; (c) N. L. Fry and P. K. Mascharak *Acc. Chem. Res.* 2011, **44**, 289-298.

12 A. Levina, A. Mitra and P. A. Lay, *Metallomics* 2009, **1**, 458-470.

13 M. Korbelik, C. S. Parkins, H. Shibuya, I. Cecic, M. R. Stratford and D. J. Chapli, *Cancer*, 2002, **82**, 1835-1843.

14   B. W. Henderson, T. M. Sitnik-Busch, L. A. Vaughan, *Photochem. Photobiol.* 1990, **70**, 64-71.

15   (a) G. Di Venosa, A. Casas, H. Fukuda, C. Perotti and A. Battle, *Nitric Oxide* 2005, **13**, 155-162; (b) G. Di Venosa, C. Perotti, H. Fukuda, A. Battle and A. J. Casas, *Photochem.Photobiol. B* 2005, **80**, 195-201.

16   Y. Yamamoto, Y. Ohgari, N. Yamaki, S. Kitajima, O. Shimokawa, A. Matsui and S. Taketani, *Biochem. Biophys. Res. Commun.* 2007, **16**, 541-546.

17   (a) D. Schaniel, T. Woike, N. R. Behrnd, J. Hauser, K. Kraemer, T. Todorova and B. Delley, *Inorg. Chem.* 2009, **48**, 11399-11406; (b) D. Schaniel, T. Woike, D. Biner, K. Kraemer and H. U. Guedel, *Phys. Chem. Chem. Phys.* 2007, **9**, 5149-5157; (c) D. Schaniel, T. Woike, C. Boskovic and H. U. Gudel, *Chem. Phys. Lett.* 2004, **390**, 347-351.

18   T. E. Bitterwolf, *Inorg. Chem. Commun.* 2008, **11**, 772-773.

19   D. V. Fomitchev, P. Coppens, T. Li, K. A. Bagley, L. Chen and G. B. Richter-Addo, *Chem. Commun.* 1999, **19**, 2013-2014.

20   S. C. Da Silva and D. W. Franco, *Spectrochim. Acta, Part A* 1999, **55A**, 1515-1525.

21   J. A. Guida, E. O. Piro and P. J. Aymonino, *Inorg. Chem.* 1995, **43**, 4113-4116.

22   U. Hauser, V. Oestriech and H.D. Rohrweck, *Z. Physik A* 1977, **280**, 125-130.

23   B. Cormary, I. Malfant, M. Buron-Le Cointe, L. Toupet, B. Delley, D. Schaniel, N. Mockus, T. Woike, K. Fejfarova, V. Petricek and M. Dusek, *Acta Crystallogr. Sect. B* 2009, **65**, 612-623.

24   (a) W. V. Moreshead, O. V. Przhonska, M. V. Bondar, A. D. Kachkovski, I. H. Nayyar, A. E. Masunov, A. W. Woodward and K. D. Belfield, *J. Phys. Chem. C*, 2013, **117**, 23133-23147; (b) X. Wang, D. M. Nguyen, C. O. Yanez, L. Rodriguez, H. Y. Ahn, M. V. Bondar and K. D. Belfield, *J. Am. Chem. Soc.* 2010, **132**, 12237-12239.

25   C. Denneval, O. Moldovan, Ch. Baudequin, S. Achelle, P. Baldeck, N. Plé, M. Darabantu and Y. Ramondenc, *Eur. J. Org. Chem.* 2013, 5591-5602.

26   (a) M. Four, D. Riehl, O. Mongin, M. Blanchard-Desce, L. M. Lawson-Daku, J. Moreau, J. Chauvin, J. A. Delaire and G. Lemercier, *Phys. Chem. Chem. Phys.* 2011, **13**, 17304-17312; (b) C. Girardot, G. Lemercier, J. C. Mulatier, J. Chauvin, P. L. Baldeck and C. Andraud, *Dalton Trans.* 2007, 3421-3426.

27   (a) C. Rouxel, M. Charlot, Y. Mir, C. Frochot, O. Mongin and M. Blanchard-Desce, *New J. Chem.* 2011, **35**, 1771-1780; (b) O. Mongin, L. Porres, M. Charlot, C. Katan and M. Blanchard-Desce, *Chem. Eur. J.* 2007, **13**, 1481-1498.

28   G. Ramos-Ortíz, J. L. Maldonado, M. C. G. Hernández, M. G. Zolotukhin, S. Fomine, N. Fröhlich, U. Scherf, F. Galbrech, E. Preis, M. Salmon, J. Cárdenas and M. I. Chávez, *Polymer* 2010 , **51** , 2351-2359.

29   M. Pawlicki, H. A. Collins, R. G. Denning and H. L. Anderson, *Angew. Chem. Int. Ed.* 2009, **48**, 3244-3266.

30   B. Strehmel and V. Strehmel, in *Advances in Photochemistry*, D. C. Neckers, W. S. Jenks and Th. Wolff eds., J. Wiley & Sons, Inc. 2007, Vol. 29, pp. 111-341.

31   K. R. Justin Thomas, J. T. Lin, C. P. Chang, C. H. Chuen and C. C. Cheng, *J. Chin. Chem. Soc.* 2002, **49**, 833-840.

32   F. Kröhnke, *Synthesis*, 1976, 1-24.

33 H. Nagano, K. Enomoto, Y. Wakabayashi, G. Komiya, T. Hirano and T. Oi, *Inorg. Chem.* 2007, **46**, 1431-1439.

34 K. Karidi, A. Garoufis, A. Tsipis, N. Hadjiliadis, H. den Dulk and J. Reedijk, *Dalton Trans.* 2005, 1176-1187.

35 J. Akl, C. Billot, P. G. Lacroix, I. Sasaki, S. Mallet-Ladeira, I. Malfant, R. Arcos-Ramos, M. Romero and N. Farfán, *New J. Chem.* 2013, **37**, 3518-3527.

36 T. Hirano, K. Ueda, M. Mukaida, H. Nagao and T. Oi, *J. Chem. Soc., Dalton Trans.,* 2001, 2341-2345.

37 J. H. Enemark and R. D. Feltham, *Coord. Chem. Rev.* 1974, **13**, 339-409.

38 R. Galvao de Lima, M. Gama Sauaia, D. Bonaventura, A. C. Tedesco, L. M. Bendhack, R. Santana da Silva, *Inorg. Chim. Acta* 2006, **359**, 2543-2549.

39 D. Tsikas, *J. Chromatogr. B* 2007, **851**, 51-70.

40 A. K. Patra, M. J. Rose, K. A. Murphy, M. M. Olmstead and P. K. Mascharak, *Inorg. Chem.* 2004, **43**, 4487-4495.

41 (a) C. F. Works and P. C. Ford, *J. Am. Chem. Soc.* 2000, **122**, 7592-7593. (b) C. F. Works, C. J. Jocher, G. D. Bart, X. Bu and P. C. Ford, *Inorg. Chem.* 2002, **41**, 3728-3739.

42 J. Bordini, D. L. Hughes, J. D. da Motta Neto and C. J. da Cunha, *Inorg. Chem.* 2002, **41**, 5410-5416.

43 O. Schiemann, N. J. Turro, J. K. Barton, *J. Phys. Chem. B* 2000, **104**, 7214-7220.

44 (a) R. Hübner, B. Sarkar, J. Fiedler, S. Záliš, W. Kaim, *Eur. J. Inorg. Chem.* 2012, 3569-3576. (b) N. Chanda, B. Sarkar, S. Kar, J. Fiedler, W. Kaim, G.K. Lahiri, *Inorg. Chem.* 2004, **43**, 5128-5133.

45 R. W. Callahan and T. J. Meyer, *Inorg. Chem.* 1977, **16**, 574-581.

46 P. De, T. K. Mondal, S. M. Mobin, B. Sarkar and G. Kumar Lahiri, *Inorg. Chim. Acta* 2010, 2945-2954.

47 P. De, B. Sarkar, S. Maji, A. Kumar Das, E. Bulak, S. M. Mobin, W. Kaim and G. Kumar Lahiri, *Eur. J. Inorg. Chem.* 2009, 2702-2710.

48 M. R. Hamblin and T. N. Demidova *Proc. SPIE, Mechanism for Low-Light Therapy* 2006, **6140**, 614001-614012.

49 S. M. Treffert-Ziemelis, J. Golus, D. P. Strommen, J. R. Kincaid*, Inorg. Chem.* 1993, **32**, 3890-3894.

50 J. R. Durig, W. A. Mc Allister, J. N. Willis Jr and E. E. Mercer, *Spectrochim. Acta*, 1966, **22**, 1091-1100.

51 G. M. Sheldrick, *Acta Cryst.* 2008, **A64**, 112-122.

52 Gaussian 09, Revision D.01, M. J. Frisch, G. W. Trucks, H. B. Schlegel, G. E. Scuseria, M. A. Robb, J. R. Cheeseman, G. Scalmani, V. Barone, B. Mennucci, G. A. Petersson, H. Nakatsuji, M. Caricato, X. Li, H. P. Hratchian, A. F. Izmaylov, J. Bloino, G. Zheng, J. L. Sonnenberg, M. Hada, M. Ehara, K. Toyota, R. Fukuda, J. Hasegawa, M. Ishida, T. Nakajima, Y. Honda, O. Kitao, H. Nakai, T. Vreven, J. A. Montgomery, Jr., J. E. Peralta, F. Ogliaro, M. Bearpark, J. J. Heyd, E. Brothers, K. N. Kudin, V. N. Staroverov, R. Kobayashi, J. Normand, K. Raghavachari, A. Rendell, J. C. Burant, S. S. Iyengar, J. Tomasi, M. Cossi, N. Rega, J. M. Millam, M. Klene, J. E. Knox, J. B. Cross, V. Bakken, C. Adamo, J. Jaramillo, R. Gomperts, R. E. Stratmann,

O. Yazyev, A. J. Austin, R. Cammi, C. Pomelli, J. W. Ochterski, R. L. Martin, K. Morokuma, V. G. Zakrzewski, G. A. Voth, P. Salvador, J. J. Dannenberg, S. Dapprich, A. D. Daniels, Ö. Farkas, J. B. Foresman, J. V. Ortiz, J. Cioslowski, and D. J. Fox, Gaussian, Inc., Wallingford CT, 2009.

53   J. Tomasi, B. Mennucci, and R. Cammi, *Chem. Rev.* 2005, **105**, 2999-3093.

54   (a) P. J. Hay and W. R. Wadt, *J. Chem. Phys.* 1985, **82**, 270-283. (b) W. R. Wadt and P. J. Hay, *J. Chem. Phys.* 1985, **82**, 284-298. (c) P. J. Hay and W. R. Wadt, *J. Chem. Phys.* 1985, **82**, 299-310.

55   M. J. Rose and P. K. Mascharak, *Inorg. Chem.* 2009, **48**, 6904-6917.

56   for example: (a) M. P. Waller, H. Braun, N. Hojdis and M. Bühl, *J. Chem. Theory Comput.* 2007, **3**, 2234-2242. (b) T. Ayed, J. C. Barthelat, B. Tangour, C. Pradère, B. Donnadieu, M. Grellier and S. Sabo-Etienne, *Organometallics* 2005, **24**, 3824-3826. (c) H. Hratchian and M. C. Milleti, *J. Mol. Struct. : THEOCHEM* 2005, **340**, 119-126. (d) D. Huang, W. E. Streib, O. Eisenstein and K. G. Caulton, *Organometallics* 2000, **19**, 1967-1972.

57   P. Hirva, M. Haukka and M. Jaconen, *J. Mol. Modell.* 2008, **14**, 171-181.

58   T. Yanai, D. Tew, and N. Handy, *Chem. Phys. Lett.* 2004, **393**, 51-57.

59   C. Hatchard and C. Parker, *Proc. R. Soc. (London) A* 1956, **235**, 518-536.

60   V. Pimienta, C. Frouté, M.-H. Deniel, D. Lavabre, R. Guglielmetti and J. C. Micheau, *Journal of Photochem and Photobiol. A*, 1999, **122**, 199-204 (reference 35)

61   Program Sa3.3 written by D. Lavabre and V. Pimienta (http://cinet.chim.pagesperso-orange.fr/tele_sa/install_Sa.html).

18

Table 1   Crystal data for 4'-(2-fluorenyl)-2,2':6',2''-terpyridine (FT), and *trans*(Cl,Cl)-
           [Ru^{II}(FT)Cl$_2$(NO)](PF$_6$)

	FT	*trans*(Cl,Cl)-[Ru^{II}(FT)Cl$_2$(NO)](PF$_6$)
Chemical formula	C$_{28}$H$_{19}$N$_3$	C$_{28}$H$_{19}$Cl$_2$F$_6$N$_4$OPRu, CH$_3$OH
M	397.46	776.45
Crystal system	orthorhombic	triclinic
a (Å)	34.960(4)	10.3340(5)
b (Å)	5.9306(7)	13.0961(6)
c (Å)	9.5911(10)	13.2279(6)
α (°)	90	72.680(2)
β (°)	90	70.488(2)
γ (°)	90	67.090(2)
V (Å^3)	1988.6(4)	1525.02(13)
T (K)	180(2)	180(2)
Space group	Pna2$_1$	P-1
Z	4	2
ρ (Mg/m^3)	1.328	1.691
Reflections		
measured	14300	16406
unique	2870	4680
R$_{int}$	0.0670	0.0470
Data / parameters	2870 / 280	4680 / 428
Final R [I>2sigma(I)]		
R$_1$	0.0424	0.0594
wR$_2$	0.0806	0.1613
Largest diff. peak (hole) e.Å^{-3}	0.152 (-0.153)	1.229 (-0.994)
GOF (F^2)	1.021	1.029

Table 2   Experimental (UV-vis spectra) and computational (**DFT**) data for the
              ruthenium complexes and that of the related terpyridine ligand.

compounds	band	experimental data		computed data	
		λ (nm)	ε (M^{-1} cm^{-1})	λ (nm)	f
FT	A	309	30 800	285	1.331
		297	30 400	278	0.278
trans-[Ru^{II}(FT)Cl$_2$(NO)](PF6)	A	414	23 600	370	0.665
		~360	weak	327	0.148
		~320	weak	298	0.339
	B	282	42 250	263	0.313
				262	0.157
				253	0.087
				251	0.166
cis-[Ru^{II}(FT)Cl$_2$(NO)](PF6)	A	389	24 950	355	0.724
		~330	weak	302	0.288
	B	283	47 900	264	0.203
				254	0.163
				252	0.087
				250	0.061
				240	0.145

Table 3 Electrochemical data ($E^{1/2}$ *vs* SCE) for the $[Ru^{II}(FT)Cl_2(NO)](PF_6)$ complexes, before and after irradiation at 405 nm. Data for $[Ru^{II}(FT)_2](PF_6)_2$ and FT are given as a reference.

compounds	Before irradiation					After irradiation	
	Reduction			Oxidation		Reduction	Oxidation
	NO⁺/NO•	**NO•/NO⁻**	**FT**	**FT**	**Ru^{III}/Ru^{II}**	**Ru^{III}/Ru^{II}**	**FT**
trans(Cl,Cl)-isomer	-0.13	-0.62	-1.30 -1.65	1.85	~2.4	0.45	1.85
cis(Cl,Cl)-isomer	-0.08	-0.32	-1.21 -1.64	1.84	~2.5	0.47	1.84
$[Ru^{II}(FT)_2](PF_6)_2$			-1.19 -1.42 -1.66	1.8 – 1.9	1.27		
FT				1.85			

Table 4   Electronic transition involved in the intense low lying band of FT, *trans*-[Ru^{II}(FT)Cl$_2$(NO)]$^+$, and *cis*-[Ru^{II}(FT)Cl$_2$(NO)]$^+$, from DFT computations, with absorption maxima (λ_{max}), oscillator strengths (*f*), and main excitations involved in the configuration interaction (CI) expansions.

Compounds	transition	λ_{max}	*f*	composition of CI expansion[1]
FT	$1 \rightarrow 2$	285	1.331	$0.619 \, \chi_{104 \rightarrow 105} + 0.264 \, \chi_{104 \rightarrow 107}$
	$1 \rightarrow 3$	278	0.278	$0.604 \, \chi_{103 \rightarrow 105} + 0.217 \, \chi_{104 \rightarrow 106}$
trans-[Ru^{II}(FT)Cl$_2$(NO)]$^+$	$1 \rightarrow 7$	370	0.665	$0.588 \, \chi_{136 \rightarrow 137} + 0.232 \, \chi_{136 \rightarrow 139} - 0.201 \, \chi_{131 \rightarrow 137}$
cis-[Ru^{II}(FT)Cl$_2$(NO)]$^+$	$1 \rightarrow 7$	355	0.724	$0.504 \, \chi_{136 \rightarrow 137} + 0.314 \, \chi_{136 \rightarrow 139} + 0.210 \, \chi_{128 \rightarrow 137}$

[1] orbital 104 (105) is the HOMO (LUMO) for FT, orbital 136 (137) is the HOMO (LUMO) for *trans*-[Ru^{II}(FT)Cl$_2$(NO)]$^+$, and *cis*-[Ru^{II}(FT)Cl$_2$(NO)]$^+$.

Table 5   DFT Computational insights (changes in ruthenium-nitrogen bond length $\Delta_{\text{Ru-NO}}$ in Å, Ru-N-O angles in degrees, and population of the LUMO orbital (electron density in %) for the *cis*- and *trans*-$[Ru^{II}(FT)Cl_2(NO)]^+$ isomers.

	cis-$[Ru^{II}(FT)Cl_2(NO)]^+$	*trans*-$[Ru^{II}(FT)Cl_2(NO)]^+$
$\Delta_{\text{Ru-NO}}$	0.117 Å	0.088 Å
Ru-N-O angle	142.9 °	147.8 °
LUMO population		
Ru	19.0 %	18.1 %
$N_{(NO)}$	34.1 %	32.2 %

23

$[Ru^{II}(py)_4(Cl)(NO)]^{2+}$

$[Ru^{II}(R\text{-terpy})(Cl)_2(NO)]^{1+}$

FT

trans(Cl,Cl)-$[Ru^{II}(FT)(Cl)_2(NO)]^{1+}$

cis(Cl,Cl)-$[Ru^{II}(FT)(Cl)_2(NO)]^{1+}$

$[Ru^{II}(FT)_2]^{2+}$

Scheme 1

24
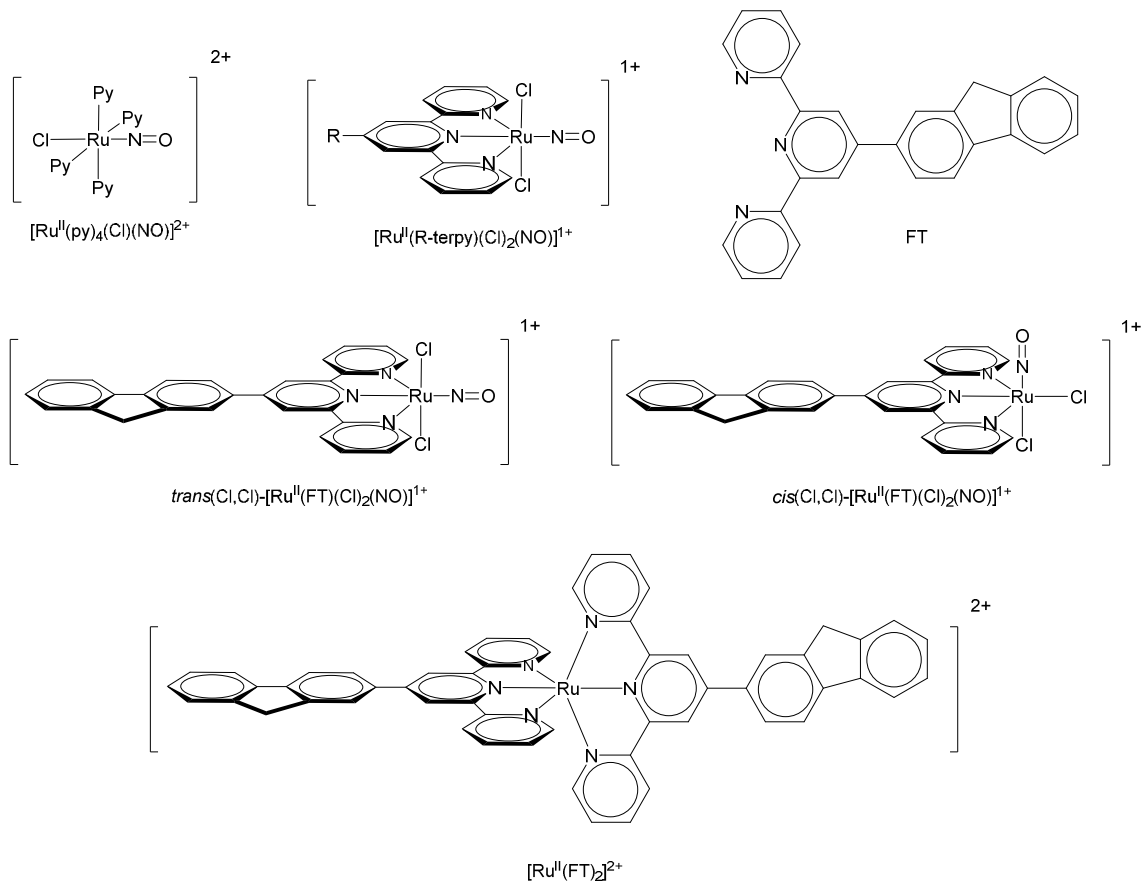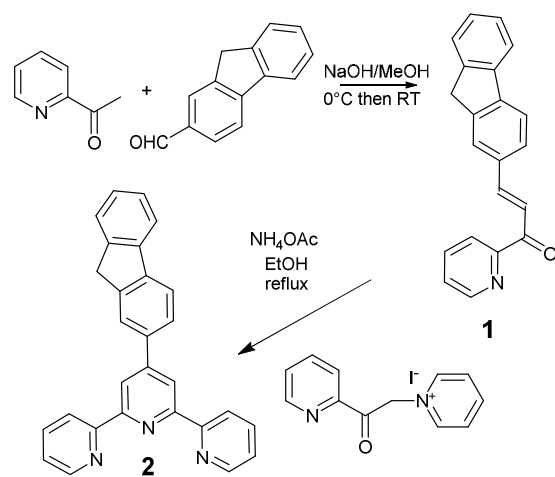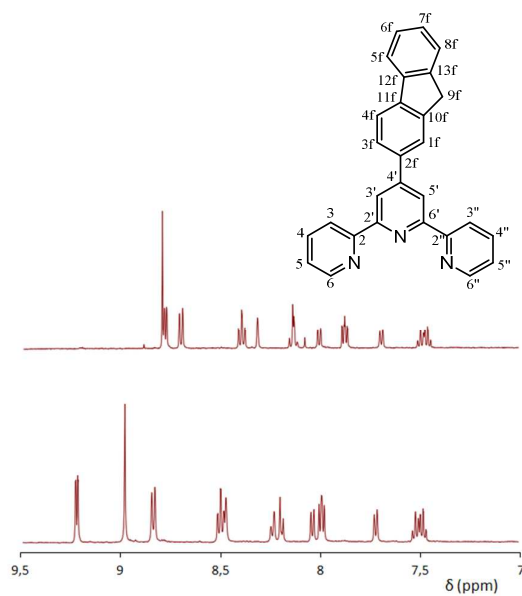
Scheme 2

Figure 1

^{1}H NMR spectra of *trans*(Cl,Cl)-[Ru^{II}(FT)Cl$_2$(NO)](PF$_6$) (top), and *cis*(Cl,Cl) [Ru^{II}(FT)Cl$_2$(NO)](PF$_6$) (bottom) in CD$_3$CN. The ligand atom labeling scheme of ligand FT is shown for the peaks assignment (see experimental section).
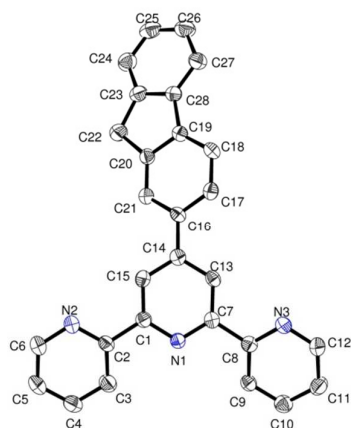
Figure 2

View of ligand FT.
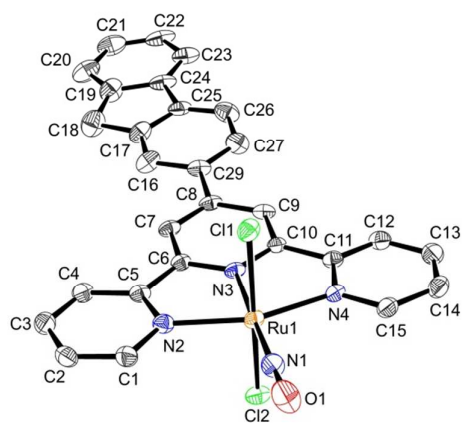
Figure 3

View of complex *trans*-[Ru^{II}(FT)Cl$_2$(NO)]$^+$.

27
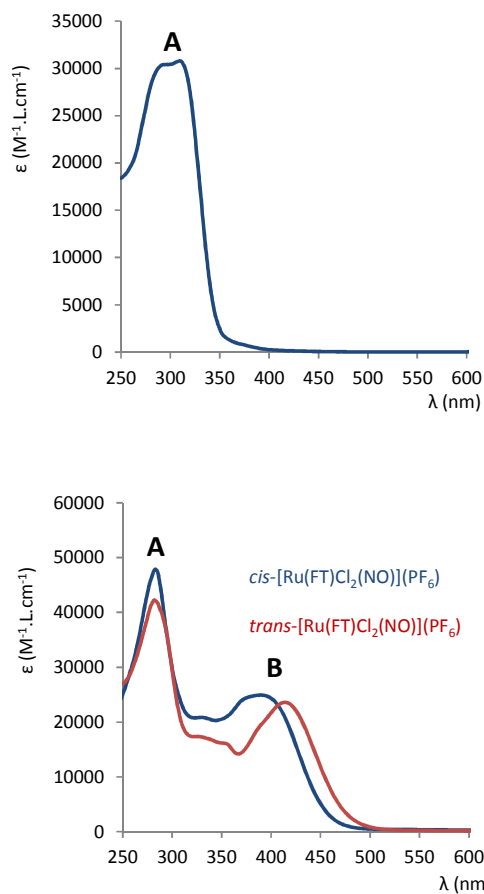
Figure 4

Experimental UV-visible spectra in acetonitrile for FT (top) and the related Ru-NO complexes (bottom), showing the main electronic features around (band **A** around 300 nm, and band **B** around 400 nm).
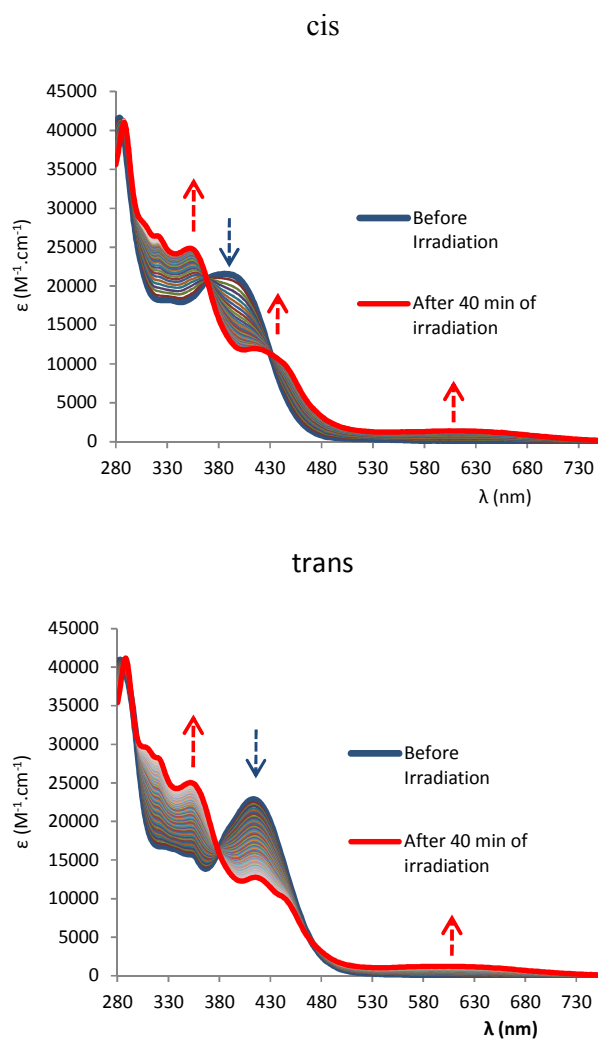
Figure 5

Changes in the absorption spectra of *cis*-[Ru^{II}(FT)Cl$_2$(NO)](PF$_6$) (top) and *trans*-[Ru^{II}(FT)Cl$_2$(NO)](PF$_6$) (bottom) in acetonitrile under irradiation at λ = 405 nm.
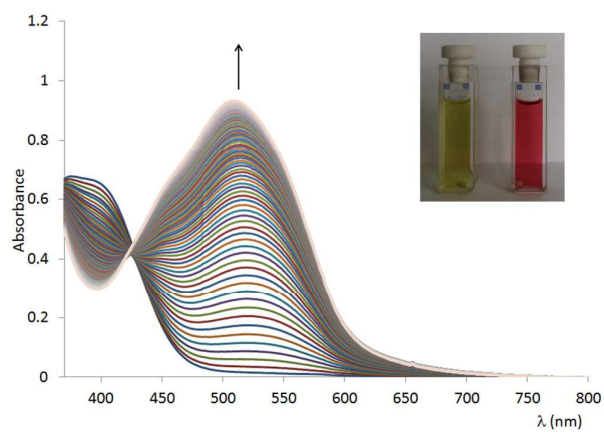
Figure 6

Electronic spectra showing the formation of azo dye when Griess reagent (1.5 mL) is added to *cis*-[Ru^{II}(FT)Cl$_2$(NO)](PF$_6$) (3.14 × 10^{-5} mol), and irradiated at λ = 405 nm at room temperature. Repetitive scans are taken every 10 sec, during 20 min. Inset: sample cell before (left) and after (right) irradiation.
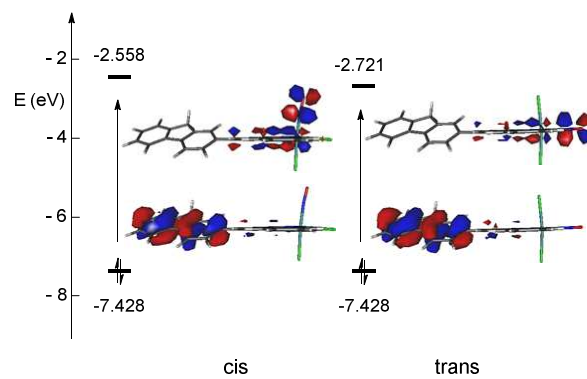
Figure 7

HOMO-LUMO (136-137) orbitals for *cis*-[Ru^{II}(FT)Cl$_2$(NO)]$^+$ (left), and *trans*-[Ru^{II}(FT)Cl$_2$(NO)]$^+$ (right).